International Journal of Solids and Structures 46 (2009) 1053–1065

Contents lists available at ScienceDirect

International Journal of Solids and Structures

journal homepage: www.elsevier.com/locate/ijsolstr

Modelling of finite piezoelectric patches: Comparing an approximate power series expansion theory with exact theory

K. Mauritsson

Department of Applied Mechanics, Chalmers University of Technology, SE-412 96 Göteborg, Sweden

ARTICLE INFO

Article history:
Received 9 June 2008
Received in revised form 17 September 2008
Available online 30 October 2008

Keywords:
Plate equations
Elastic waves
Piezoelectricity
Actuator
Power series expansions
Equivalent boundary condition
Exact solution

ABSTRACT

Plate equations for a plate consisting of one elastic layer and one piezoelectric layer with an applied electric voltage have previously been derived by use of power series expansions of the field variables in the thickness coordinate. These plate equations are here evaluated by the consideration of a time harmonic 2D vibration problem with finite layers. The boundary conditions at the sides of the layers then have to be considered. Numerical comparisons of the displacement field are made with solutions from two other theories; a solution with equivalent boundary conditions for a thin piezoelectric layer applied on an elastic plate and an exact solution based on Fourier series expansions. The two approximate theories are shown to be equally good and they both yield accurate results for low frequencies and thin plates.

1. Introduction

The use of piezoelectric layers in engineering applications for sensing and actuation purposes has been the subject of much research in recent years. As the piezoelectric layer and the structure to which it is attached are usually thin in comparison to relevant wavelengths it is natural to develop beam, plate and shell equations for layered structures including piezoelectric layers. Many references to work prior to 2000 are given by the review articles by Gopinathan et al. (2000) and Wang and Yang (2000). Bisegna and Caruso (2001) present a classification and critical comparison among higher-order piezoelectric plate models based on power series expansions prior to 2001. Also many investigations in recent years concern the modelling of layered piezoelectric structures based on power series expansions of some small parameter; a few references are given here (Lim and Lau, 2005; Fernandes and Pouget, 2002, 2006; Kapuria, 2004; Kapuria and Achary, 2005; Lim et al., 2006; Wu and Lo, 2006). The finite element method is developed for such problems in, e.g., Kögl and Bucalem (2005), Vasques and Rodrigues (2005), Robbins and Chopra (2006). The exact three-dimensional solution of problems with piezoelectric actuators and sensors attached on elastic bodies are treated by e.g., Kochetkov and Rogacheva (2005) and Raghavan and Cesnik (2005).

Recently Mauritsson et al. (2008) have derived plate equations for a layered plate consisting of one orthotropic elastic layer and one piezoelectric layer of class *2mm* with specified electric potential at the bottom and the top. In the derivation all field quantities in both layers are expanded in power series in the thickness coordinate. Insertion into the three-dimensional equations of motion gives recursion relations among the expansion functions which can be used to eliminate all but some of the lowest order expansion functions. The boundary and interface conditions then give a set of equations which is eliminated to six plate equations for the elastic layer. Three of these correspond to the symmetric (in the limit of vanishing piezoelectric layer) part of the motion and are truncated to linear order in the thickness. The other three equations correspond to the antisymmetric (in the limit of vanishing piezoelectric layer) part of the motion and are truncated to quadratic order in the thickness. In that study the plate equations are evaluated by some numerical comparisons with exact theory, but only the case of an infinite plate is considered. The purpose of this paper is to further evaluate the plate equations derived in Mauritsson et al. (2008) by considering the case of a finite plate consisting of two layers of different lengths. To do this the displacement field in the elastic layer for a 2D time harmonic problem, described in Section 2, is investigated. As the layers are of finite lengths now also the boundary conditions at the ends of the layers are specified. The set of boundary conditions to combine with the plate equations are then derived by inserting the power series expansions of the displacements into the physical conditions at the sides of

E-mail address: karl.mauritsson@chalmers.se

0020-7683/$ - see front matter © 2008 Elsevier Ltd. All rights reserved.
doi:10.1016/j.ijsolstr.2008.10.022

the elastic layer and identifying equal powers of the thickness coordinate. This procedure and the determination of the displacement field is described in Section 3. To evaluate the plate equations comparisons are made with solutions from two other theories; a solution with equivalent boundary conditions for a thin piezoelectric layer applied on an elastic plate, described in Section 4, and an exact solution, described in Section 5. The equivalent boundary conditions are derived by Johansson and Niklasson (2003) using the same type of series expansions as in the derivation of the plate equations. In the solution with equivalent boundary conditions no equations of motion for the piezoelectric layer have to be considered at all. The piezoelectric layer instead comes in as source terms in the plate equations for the elastic plate, which are taken from Boström et al. (2001). Also the derivation of these plate equations are based on the same series expansion approach. The exact solution of the problem follows an approach based on Fourier series expansions, similar to one adopted by Boström and Zhang (2005) for a piezoelectric strip actuator. In Section 6 numerical calculations of the displacement field are compared between the three theories. The two approximate theories are shown to be equally good and they both yield accurate results for low frequencies and thin plates as long as the piezoelectric layer is thin in comparison to the total plate thickness.

2. Problem formulation

Consider a plate with two symmetrically placed finite layers according to Fig. 1. The upper piezoelectric layer has thickness h_p and length $2L_p$, while the lower elastic layer has thickness h_e and length $2L_e$. A coordinate system is introduced with the x axis along the interface between the two layers. The piezoelectric layer is assumed to be a hexagonal, transversely isotropic material (6 mm) and the elastic layer is isotropic. Only time harmonic vibrations in the xz plane are considered and there is no y dependence. The time factor $e^{-i\omega t}$, where ω is the angular frequency and t is the time, is suppressed throughout.

Below, the governing equations for the upper layer, which consists of a piezoelectric material of class 6 mm, are given. The material can then be specialized to be isotropic elastic, as in the lower layer. The quasistatic approximation is made, which means that no magnetic fields are involved. Displacements in the x and z direction are denoted by u and w, respectively. The mechanical fields in the piezoelectric layer are given an upper index 'p' to distinguish them from corresponding fields in the elastic layer. The electric potential is denoted by Φ. The piezoelectric material has density ρ_p while the elastic material has density ρ_e. The non-standard notation k_{ij} is used for the stiffness constants in the piezoelectric layer as this notation is used in Mauritsson et al. (2008), where the standard notation c_{ij} is used for the stiffness constants in the elastic layer. Here the elastic layer consists of an isotropic elastic material, so the stiffnesses in this layer are expressed in terms of the Lamé constants, λ and μ. The piezoelectric coupling constants are denoted by e_{ij} and the dielectric constants are ϵ_{ij}.

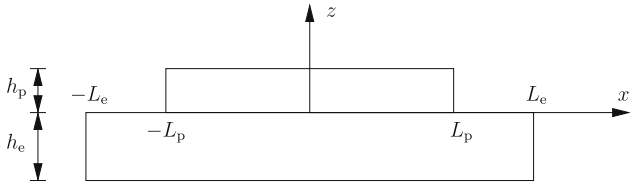

Fig. 1. The geometry with a two-layered plate.

The stress components of the piezoelectric layer are

$$T^p_{xx} = k_{11}\partial_x u^p + k_{13}\partial_z w^p + e_{z1}\partial_z \Phi, \tag{2.1}$$

$$T^p_{xz} = k_{44}(\partial_z u^p + \partial_x w^p) + e_{x5}\partial_x \Phi, \tag{2.2}$$

$$T^p_{zz} = k_{13}\partial_x u^p + k_{33}\partial_z w^p + e_{z3}\partial_z \Phi, \tag{2.3}$$

and the electric displacement components are

$$D_x = e_{x5}(\partial_z u^p + \partial_x w^p) - \epsilon_{xx}\partial_x \Phi, \tag{2.4}$$

$$D_z = e_{z1}\partial_x u^p + e_{z3}\partial_z w^p - \epsilon_{zz}\partial_z \Phi, \tag{2.5}$$

where partial derivatives with respect to x and z are denoted by ∂_x and ∂_z, respectively.

The three equations of motion for the piezoelectric layer become

$$k_{11}\partial_x^2 u^p + k_{44}\partial_z^2 u^p + (k_{13}+k_{44})\partial_x\partial_z w^p + (e_{x5}+e_{z1})\partial_x\partial_z \Phi = -\rho_p \omega^2 u^p, \tag{2.6}$$

$$k_{44}\partial_x^2 w^p + k_{33}\partial_z^2 w^p + (k_{13}+k_{44})\partial_x\partial_z u^p + e_{x5}\partial_x^2 \Phi + e_{z3}\partial_z^2 \Phi = -\rho_p \omega^2 w^p, \tag{2.7}$$

$$e_{x5}\partial_x^2 w^p + e_{z3}\partial_z^2 w^p + (e_{x5}+e_{z1})\partial_x\partial_z u^p - \epsilon_{xx}\partial_x^2 \Phi - \epsilon_{zz}\partial_z^2 \Phi = 0. \tag{2.8}$$

The governing equations in the isotropic elastic layer can be obtained as a special case of the equations above by putting all electric fields and all the piezoelectric coupling constants to zero.

The boundary and interface conditions must now be specified. The approximate plate equations, which are going to be treated in the following section, are applicable to a free plate where the piezoelectric layer is working as an actuator, i.e. the electric potential is specified on the top and the bottom of the piezoelectric layer.

At the free bottom surface of the elastic layer the stress vector vanishes:

$$T_{xz} = 0, \quad |x| \leqslant L_e, \quad z = -h_e, \tag{2.9}$$

$$T_{zz} = 0, \quad |x| \leqslant L_e, \quad z = -h_e. \tag{2.10}$$

Also at the top of the piezoelectric layer the stress vector vanishes and in addition the electric potential is specified:

$$T^p_{xz} = 0, \quad |x| \leqslant L_p, \quad z = h_p, \tag{2.11}$$

$$T^p_{zz} = 0, \quad |x| \leqslant L_p, \quad z = h_p, \tag{2.12}$$

$$\Phi = V_1, \quad |x| \leqslant L_p, \quad z = h_p. \tag{2.13}$$

At $z = 0$ the interface conditions between the two layers involve the continuity of stress and displacement and outside the interface the top of the elastic layer is free:

$$T_{xz} = \begin{cases} T^p_{xz}, & |x| \leqslant L_p \\ 0, & L_p < |x| \leqslant L_e \end{cases}, \quad z = 0, \tag{2.14}$$

$$T_{zz} = \begin{cases} T^p_{zz}, & |x| \leqslant L_p \\ 0, & L_p < |x| \leqslant L_e \end{cases}, \quad z = 0, \tag{2.15}$$

$$u = u^p, \quad |x| \leqslant L_p, \quad z = 0, \tag{2.16}$$

$$w = w^p, \quad |x| \leqslant L_p, \quad z = 0. \tag{2.17}$$

On the bottom of the piezoelectric layer the electric potential is specified:

$$\Phi = V_0, \quad |x| \leqslant L_p, \quad z = 0. \tag{2.18}$$

The applied electric potentials V_0 at the interface and V_1 at the top of the piezoelectric layer are space-independent.

Here the case of finite layers are going to be considered, which means that also boundary conditions at the sides of the layers have to be specified. On the sides of the elastic layer the boundary conditions are chosen as

$$u = 0, \quad x = \pm L_e, \quad -h_e \leqslant z \leqslant 0, \tag{2.19}$$

$$T_{xz} = 0, \quad x = \pm L_e, \quad -h_e \leqslant z \leqslant 0. \tag{2.20}$$

On the sides of the piezoelectric layer there are no electrodes and an approximate boundary condition for this is, see Tiersten (1969):

$$D_x = 0, \quad x = \pm L_p, \quad 0 \leqslant z \leqslant h_p. \tag{2.21}$$

The mechanical boundary conditions at the sides of the piezoelectric layer are chosen as for the elastic layer, i.e.

$$u^p = 0, \quad x = \pm L_p, \quad 0 \leqslant z \leqslant h_p, \tag{2.22}$$

$$T^p_{xz} = 0, \quad x = \pm L_p, \quad 0 \leqslant z \leqslant h_p. \tag{2.23}$$

The choice of mechanical boundary conditions at the sides of the layers, Eqs. 2.19, 2.20, 2.22 and 2.23, also used by Gopinathan et al. (2000) and Boström and Zhang (2005), have the advantage that they, together with the electric boundary condition (2.21), make it possible to expand the fields inside the two layers in simple trigonometric series in x. This is used in the exact solution of the problem in Section 5.

3. Plate equations

In Mauritsson et al. (2008) a set of six equations is derived for a plate consisting of two layers. The lower layer consists of an orthotropic elastic material and the upper one of a piezoelectric material of class *2mm* poled in the normal direction. The electric potentials on the bottom and the top of the piezoelectric layer are specified and can be arbitrary functions of time. All stresses are zero at the free top and bottom of the layered plate.

Here the approximate plate equations are used to solve the 2D problem described in Section 2. Therefore all displacements in the y direction are zero and there are no y-dependence in the fields. The system of six equations then reduces to a set of only four equations. Assuming time harmonic conditions the four plate equations take the following form, see Mauritsson et al. (2008):

$$\begin{aligned} &A_{00}u_0 + A_{02}\partial_x^2 u_0 + A_{01}\partial_x w_1 \\ &\quad + \alpha h_e[A_{10}u_1 + A_{12}\partial_x^2 u_1 + A_{11}\partial_x w_0 + A_{13}\partial_x^3 w_0] = 0, \end{aligned} \tag{3.1}$$

$$B_{00}w_1 + B_{01}\partial_x u_0 + \alpha h_e[B_{10}w_0 + B_{12}\partial_x^2 w_0 + B_{11}\partial_x u_1] = \alpha h_e b_1 \Delta V, \tag{3.2}$$

$$\begin{aligned} &C_{00}u_1 + C_{01}\partial_x w_0 + \alpha h_e[C_{10}u_0 + C_{12}\partial_x^2 u_0 + C_{11}\partial_x w_1] \\ &\quad + h_e^2[C_{20}u_1 + C_{22}\partial_x^2 u_1 + C_{21}\partial_x w_0 + C_{23}\partial_x^3 w_0] = 0, \end{aligned} \tag{3.3}$$

$$\begin{aligned} &D_{00}w_0 + D_{02}\partial_x^2 w_0 + D_{01}\partial_x u_1 \\ &\quad + \alpha h_e[D_{10}w_1 + D_{12}\partial_x^2 w_1 + D_{11}\partial_x u_0 + D_{13}\partial_x^3 u_0] \\ &\quad + h_e^2[D_{20}w_0 + D_{22}\partial_x^2 w_0 + D_{24}\partial_x^4 w_0 + D_{21}\partial_x u_1 + D_{23}\partial_x^3 u_1] \\ &\quad = \alpha d_0 \Delta V + \alpha^3 h_e^2 d_2 \Delta V, \end{aligned} \tag{3.4}$$

where $\Delta V = V_1 - V_0$ is the applied electric potential across the piezoelectric layer and the constant $\alpha = h_p/h_e$ is the thickness ratio between the layers. The constants A_{ij}, B_{ij}, C_{ij} and D_{ij} are depending on the materials, the thickness ratio α and the frequency, while the constants b_i and d_i are only depending on the materials and the frequency (see Mauritsson et al. (2008) for the explicit expressions). The four equations contain the unknown field variables in the elastic layer u_0, u_1, w_0 and w_1. The displacements in the elastic layer are given by the following power series expansions, see Mauritsson et al. (2008)

$$u(x,z) = u_0(x) + zu_1(x) + z^2u_2(x) + \cdots, \tag{3.5}$$

$$w(x,z) = w_0(x) + zw_1(x) + z^2w_2(x) + \cdots. \tag{3.6}$$

All expansion functions with index $j = 2, 3, \ldots$, can be expressed in those with index $j = 0$ and $j = 1$ by using recursion relations given in Mauritsson et al. (2008). The z coordinate refers to a coordinate system with origin in the middle of the elastic layer, which is another placement of coordinate system than the placement in Fig. 1. Eqs. (3.1) and (3.2) are given to linear order in h_e and correspond to the symmetric (in the limit of vanishing piezoelectric layer) part of the motion, while Eqs. (3.3) and (3.4) are given to quadratic order in h_e and correspond to the antisymmetric part of the motion.

As the problem is symmetric in x, only the half plate, $x \geqslant 0$, is considered. Furthermore, the two layers in the current problem are of different lengths. To be able to use the approximate plate equations it is therefore necessary to divide the plate in two parts, one plate with two layers for $0 \leqslant x \leqslant L_p$ and one plate consisting of only one elastic layer for $L_p < x \leqslant L_e$. In both intervals the four plate equations can be used, but in the purely elastic interval the thickness ratio α is put to zero. This results in four equations of the same form as Eqs. (3.1)–(3.4), but with no linear terms in h_e and no source terms. Use an upper index '(1)' for mechanical fields in the elastic layer for $0 \leqslant x \leqslant L_p$ and an upper index '(2)' for mechanical fields in the elastic layer for $L_p < x \leqslant L_e$. Collect the displacements in vectors like

$$\mathbf{u}^{(1)} = \begin{pmatrix} u_0^{(1)} \\ w_1^{(1)} \\ w_0^{(1)} \\ u_1^{(1)} \end{pmatrix}, 0 \leqslant x \leqslant L_p, \mathbf{u}^{(2)}_{\text{sym}} = \begin{pmatrix} u_0^{(2)} \\ w_1^{(2)} \end{pmatrix}, \mathbf{u}^{(2)}_{\text{asym}} = \begin{pmatrix} w_0^{(2)} \\ u_1^{(2)} \end{pmatrix}, \quad L_p < x \leqslant L_e.$$

To find the homogenous solution in the piezoelectric interval, $\mathbf{u}^{(1)} = e^{\lambda x}\mathbf{a}$ is inserted into Eqs. (3.1)–(3.4) with no source terms. This gives a homogenous system of four equations in the four unknowns $a_1, \ldots, a_4$, which are the components of $\mathbf{a}$. Non-trivial solutions require that the system determinant is zero and this gives an equation of the eighth degree in λ. For each solution λ_j, $j = 1, \ldots, 8$, the corresponding $(a_1)_j, \ldots, (a_4)_j$, can then be solved for. A particular solution is found by inserting a constant field $\mathbf{K}$ into Eqs. (3.1)–(3.4) and solving. The general solution for the mechanical field in the piezoelectric interval can then be written

$$\mathbf{u}^{(1)} = \sum_{j=1}^{8} A_j e^{\lambda_j x}\mathbf{a}_j + \mathbf{K}, \tag{3.7}$$

where A_j, $j = 1, \ldots, 8$, are constants to be determined.

The solution in the elastic interval is determined in an analogous way. As the linear terms in h_e vanish when the piezoelectric thickness is put to zero, Eqs. (3.1)–(3.4) decouple into two symmetric and two antisymmetric homogenous equations. For the symmetric motion $\mathbf{u}^{(2)}_{\text{sym}} = e^{kx}\mathbf{b}$ is inserted into Eqs. (3.1) and (3.2) with vanishing piezoelectric layer and for the antisymmetric motion $\mathbf{u}^{(2)}_{\text{asym}} = e^{\mu x}\mathbf{c}$ is inserted into Eqs. (3.3) and (3.4) with vanishing piezoelectric layer. There will then be two solutions for k and four solutions for μ, so the solutions in the elastic interval can be written

$$\mathbf{u}^{(2)}_{\text{sym}} = \sum_{j=1}^{2} B_j e^{k_j x}\mathbf{b}_j, \quad \mathbf{u}^{(2)}_{\text{asym}} = \sum_{j=1}^{4} C_j e^{\mu_j x}\mathbf{c}_j, \tag{3.8}$$

where B_j, $j = 1, 2$, and C_j, $j = 1, \ldots, 4$, are constants to be determined.

There are a total of 14 unknown constants and therefore a total of 14 conditions have to be specified at $x = 0$, $x = L_p$ and $x = L_e$. These conditions are derived by inserting the power series expansions of the displacements, Eqs. (3.5) and (3.6), into the physical conditions at the sides of the elastic layer and the interface between the plates. As these conditions shall be fulfilled for all z, equal powers of z are identified and each physical condition then gives an infinite number of conditions on the displacements and their derivatives. For the

almost symmetric part of the motion the most important expansion functions are the even ones for the horizontal displacement u and the odd ones for the vertical displacement w, see Eqs. (3.5) and (3.6), as the other ones correspond to the coupling to the antisymmetric motion. For the almost antisymmetric part of the motion the most important expansion functions are the odd ones for u and the even ones for w, as the other ones correspond to the coupling to the symmetric motion. As the almost symmetric equations are given to linear order in h_e and the almost antisymmetric equations are given to quadratic order, only conditions that involve no other symmetric expansion functions than u_0 and w_1 and no other antisymmetric expansion functions than u_1, w_0 and w_2 are kept. Furthermore, as only expansion functions for u up to linear order are used, only conditions up to linear order in z are kept. To express w_2 in terms of w_0 and u_1 a recursion relation from Mauritsson et al. (2008) is used:

$$w_2 = -\frac{1}{2(\lambda+2\mu)}[\rho_e\omega^2 w_0 + \mu\partial_x^2 w_0 + (\lambda+\mu)\partial_x u_1]. \tag{3.9}$$

The described method of selection results in 14 conditions and these are given below. Notice that the selection method is purely mathematical, but after the selection is made the conditions can be given a physical interpretation, which is also done.

At the left side of the half plate, i.e. at the middle of the total plate, at $x = 0$, two physical symmetry conditions can be stated. The horizontal displacement, $u^{(1)}$, and the angle, $\partial_x w^{(1)}$, are zero. Inserting the power series expansion (3.5) into the condition $u^{(1)} = 0$, keeping terms up to linear order and identifying equal powers of z gives the following two equations:

$$u_0^{(1)} = 0, \quad x = 0, \tag{3.10}$$

$$u_1^{(1)} = 0, \quad x = 0. \tag{3.11}$$

The condition $\partial_x w^{(1)} = 0$ gives

$$\partial_x w_0^{(1)} = 0, \quad x = 0, \tag{3.12}$$

$$\partial_x w_1^{(1)} = 0, \quad x = 0. \tag{3.13}$$

The physical interpretation of the symmetry condition (3.10), which is connected to the rod-like almost symmetric part of the motion, is that the horizontal displacement in the middle of the elastic layer is zero. Eqs. (3.11) and (3.12) are connected to the beam-like almost antisymmetric part of the motion and these two equations together correspond to zero angle in the middle of the elastic layer and zero shear force. Eq. (3.13) is connected to the symmetric part, but here no obvious physical interpretation can be done. One interpretation, however, is that the shear stress is zero at every point along the symmetry line.

At the right end of the plate, at $x = L_e$, the horizontal displacement, $u^{(2)}$, and the shear stress, $T_{xz}^{(2)}$, are zero. The condition $u^{(2)} = 0$ gives

$$u_0^{(2)} = 0, \quad x = L_e, \tag{3.14}$$

$$u_1^{(2)} = 0, \quad x = L_e. \tag{3.15}$$

The condition $T_{xz}^{(2)} = 0$ gives

$$u_1^{(2)} + \partial_x w_0^{(2)} = 0, \quad x = L_e. \tag{3.16}$$

Observe that in the last condition only the lowest order term is kept as the linear term involves u_2. Eq. (3.14) corresponds to zero horizontal displacement in the middle of the layer, while Eqs. (3.15) and (3.16) together represent zero angle in the middle of the layer and zero shear force.

At the interface between the piezoelectric and elastic interval, at $x = L_p$, continuity of the two displacement components and the two stress components has to be satisfied. Continuity of horizontal displacement, $u^{(1)} = u^{(2)}$, gives

$$u_0^{(1)} = u_0^{(2)}, \quad x = L_p, \tag{3.17}$$

$$u_1^{(1)} = u_1^{(2)}, \quad x = L_p. \tag{3.18}$$

Continuity of vertical displacement, $w^{(1)} = w^{(2)}$, gives

$$w_0^{(1)} = w_0^{(2)}, \quad x = L_p, \tag{3.19}$$

$$w_1^{(1)} = w_1^{(2)}, \quad x = L_p. \tag{3.20}$$

Continuity of normal stress, $T_{xx}^{(1)} = T_{xx}^{(2)}$, gives

$$(\lambda+2\mu)\partial_x u_0^{(1)} + \lambda w_1^{(1)} = (\lambda+2\mu)\partial_x u_0^{(2)} + \lambda w_1^{(2)}, \quad x = L_p, \tag{3.21}$$

$$\mu(3\lambda+4\mu)\partial_x u_1^{(1)} - \rho_e\omega^2\lambda w_0^{(1)} - \lambda\mu\partial_x^2 w_0^{(1)} = \mu(3\lambda+4\mu)\partial_x u_1^{(2)} - \rho_e\omega^2\lambda w_0^{(2)} - \lambda\mu\partial_x^2 w_0^{(2)}, \quad x = L_p. \tag{3.22}$$

Continuity of shear stress, $T_{xz}^{(1)} = T_{xz}^{(2)}$, gives

$$u_1^{(1)} + \partial_x w_0^{(1)} = u_1^{(2)} + \partial_x w_0^{(2)}, \quad x = L_p. \tag{3.23}$$

Only the lowest order term is kept in the last condition as the linear term involves u_2. Eqs. 3.17, 3.20 and 3.21 are symmetric interface conditions, where Eq. (3.17) corresponds to continuity of horizontal displacement in the middle of the elastic layer, Eq. (3.20) has no obvious interpretation, but can be seen as continuity of vertical displacement for all points along the interface, and Eq. (3.21) corresponds to continuity of normal force. Eqs. 3.18, 3.19, 3.22 and 3.23 are antisymmetric interface conditions, where Eq. (3.18) together with Eq. (3.23) represent continuity of angle in the middle of the elastic layer and continuity of shear force, Eq. (3.19) corresponds to continuity of vertical displacement in the middle of the elastic layer and Eq. (3.22) corresponds to continuity of bending moment.

Eqs. (3.10)–(3.23) are the 14 conditions needed for the determination of the 14 unknown constants. Insertion of Eqs. (3.7) and (3.8) into Eqs. (3.10)–(3.23) gives a linear system of equations and the constants can then be solved for. The displacement fields are then given by Eqs. (3.7) and (3.8).

It can be noticed that there are two conditions without any obvious physical interpretation, Eqs. (3.13) and (3.20), belonging to the interval with a piezoelectric layer on top of the elastic layer. This kind of conditions are only needed when there is a coupling between the symmetric and antisymmetric motion, so they do not arise among the boundary conditions at the end of the one-layered elastic plate. Furthermore, it should be noticed that by using the derived symmetry, boundary and interface conditions for the elastic layer, Eqs. (3.10)–(3.23), the actual symmetry and boundary conditions at the sides of the piezoelectric layer are not taken into account at all. However, it is believed that the mechanical and electrical symmetry and boundary conditions for the piezoelectric layer do not affect the result that much, especially when the piezoelectric layer is thin. It is possible to derive an alternative set of boundary conditions by establishing the physical conditions at the boundaries of both the elastic and the piezoelectric layer and insert the power series expansions of all field quantities. Identification of equal powers of the vertical coordinate then gives an infinite number of conditions. The conditions that involve the piezoelectric field variables can then be expressed in the elastic field variables, by use of the interface conditions between the two layers, established in Mauritsson et al. (2008). Boundary conditions up to some order in the vertical coordinate are kept until there are just as many equations as unknowns. However, this set of boundary conditions will not give any better results as some of the important conditions on the boundaries of the elastic layer now have to be left out. It is also more natural to only use conditions on the elastic layer as the plate equations only refers to displacements in the elastic layer.

4. Equivalent boundary conditions

For comparison, the problem described in Section 2 is here solved with a combination of two other approximate theories based on the same type of series expansions as the plate equations described in the previous section. The elastic layer is described by the approximate antisymmetric plate equations for a homogenous, isotropic, elastic plate derived by Boström et al. (2001), similar to the Mindlin plate equations, see Mindlin (1951). The derivation is made by expanding the displacements in antisymmetric power series in the thickness coordinate. Insertion in the three-dimensional equations of motion gives recursion relations which are inserted into the expanded boundary conditions at the top and the bottom of the plate. This results in plate equations which can be truncated to any order.

The piezoelectric layer comes in as source terms for $|x| \leqslant L_p$, which are modeled by the equivalent boundary conditions for a thin piezoelectric layer working as a 2D actuator on an elastic half space, derived by Johansson and Niklasson (2003). In this derivation the displacements and the electric potential in the piezoelectric layer are expanded in the thickness coordinate. This leads to recursion relations which can be inserted into the expanded boundary conditions at the top and the bottom of the piezoelectric plate. The boundary conditions on the bottom include displacements and stresses at the top of the elastic half-space. From the boundary conditions all piezoelectric expansion functions can be eliminated and the stresses at the top of the elastic layer can be expressed in the displacements at the top of this layer, the applied electric voltage and some material constants belonging to the piezoelectric layer. These expressions are power series expansions in the piezoelectric layer thickness and truncation gives the equivalent boundary conditions for the top of the elastic layer.

As the elastic plate equations in Boström et al. (2001) describe the antisymmetric part of the motion, also the applied surface traction is presupposed to be antisymmetric. This means that the situation described in Section 2 can not be modeled directly by these equations. Instead it is assumed that the two-layered plate can be replaced by a three-layered plate with an elastic layer in the middle and a piezoelectric layer of half the original thickness on both the top and the bottom of the middle layer, see Fig. 2. The two piezoelectric layers are identical and symmetrically placed. The potential V_1 is applied on the top of both layers and the potential V_0 is applied on the bottom of both layers. This antisymmetric problem with two thinner piezoelectric layers is assumed to give approximately the same displacements in the elastic layer as the original problem with just one thicker piezoelectric layer on top of the elastic one.

As the problem is symmetric in x, only the half plate, $x \geqslant 0$, is considered. Furthermore, the plate is divided into two intervals, as in the previous section. The first interval, $0 \leqslant x \leqslant L_p$, has source terms described by the equivalent boundary conditions, while the other interval, $-L_p < x \leqslant L_e$, has no source terms. Both parts of the elastic plate are described by the following two plate equations, taken from Boström et al. (2001), truncated to quadratic order and specialized to a time harmonic 2D case with no displacements in the y direction and all partial derivatives with respect to y put to zero:

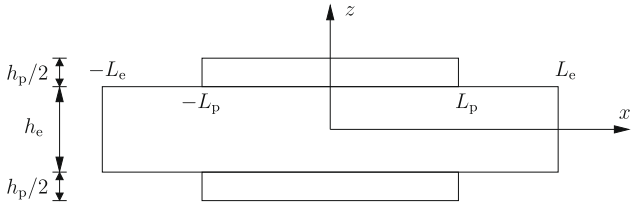

Fig. 2. The equivalent boundary conditions geometry with a three-layered plate.

$$u_1 + \partial_x w_0 - \frac{h_e^2}{8}\left[\frac{\omega^2}{c_s^2}u_1 + (3-2\gamma)\partial_x^2 u_1 - (1-2\gamma)\left(\frac{\omega^2}{c_s^2}\partial_x w_0 + \partial_x^3 w_0\right)\right] = \frac{T_x}{\mu}, \quad (4.1)$$

$$-\frac{h_e}{2}\left[\partial_x u_1 + \frac{\omega^2}{c_s^2}w_0 + \partial_x^2 w_0\right] + \frac{h_e^3}{48}\left[\frac{2-\gamma}{c_s^2}\omega^2\partial_x u_1 + (3-2\gamma)\partial_x^3 u_1 + \frac{\gamma}{c_s^4}\omega^4 w_0 - \frac{1-3\gamma}{c_s^2}\omega^2\partial_x^2 w_0 - (1-2\gamma)\partial_x^4 w_0\right] = \frac{P}{\mu}, \quad (4.2)$$

Here $c_s = \sqrt{\mu/\rho_e}$ is the transverse wave speed and $\gamma = \mu/(\lambda+2\mu)$ is the squared quotient between the transverse and longitudinal wave speeds. The source terms T_x and P are the applied shear and normal stresses at the top of the elastic layer. Observe that, due to antisymmetry, T_x and $-P$ are the applied shear and normal stresses at the bottom of the plate. The two plate equations contain two unknown field variables, u_1 and w_0, which are defined by the following power series expansions, using a coordinate system with origin in the middle of the elastic layer

$$u(x,z) = z u_1(x) + z^3 u_3(x) + \cdots, \quad (4.3)$$

$$w(x,z) = w_0(x) + z^2 w_2(x) + \cdots. \quad (4.4)$$

As the motion is assumed to be antisymmetric, the series expansion of the horizontal displacement u only includes odd expansion functions, while the series expansion of the vertical displacement w only includes even ones. Observe that in Boström et al. (2001) the elastic layer thickness is $2h$, while here the thickness is h_e, which explains some modifications in the plate equations taken from there.

For $0 \leqslant x \leqslant L_p$, the stresses at the top of the elastic layer are taken from Johansson and Niklasson (2003):

$$T_x = \frac{h_p}{2}\left[\rho_p\omega^2 + \left(k_{11} - \frac{k_{13}^2}{k_{33}}\right)\partial_x^2\right]u|_{z=h_e/2}, \quad (4.5)$$

$$P = \frac{h_p\rho_p\omega^2}{2}\left[w|_{z=h_e/2} - \frac{e_{z3}}{2k_{33}}\Delta V\right]. \quad (4.6)$$

Observe that the thicknesses of the two piezoelectric layers are $h_p/2$, which explains some modifications in the equivalent boundary conditions taken from Johansson and Niklasson (2003). The displacements at the top of the elastic layer, $u|_{z=h_e/2}$ and $w|_{z=h_e/2}$, are determined from the series expansions (4.3) and (4.4), respectively. Insertion of Eqs. (4.5) and (4.6), with $h_p = \alpha h_e$, into Eqs. (4.1) and (4.2) then gives two plate equations which are truncated to quadratic order in h_e. These equations include the expansion functions w_0, u_1 and w_2, where w_2 is expressed in terms of w_0 and u_1 with a recursion relation from Boström et al. (2001), which is actually the same as Eq. (3.9). Two plate equations in the two unknown expansion functions, w_0 and u_1, are obtained and given below. These equations describe the situation for $0 \leqslant x \leqslant L_p$, while for $L_p < x \leqslant L_e$ the same equations are used but with $\alpha = 0$, which gives two simpler equations with no source terms:

$$\mu(u_1 + \partial_x w_0) - \frac{h_e^2}{8}\left[(\rho_e + 2\alpha\rho_p)\omega^2 u_1 + \left(\frac{\mu(3\lambda+4\mu)}{\lambda+2\mu} + 2\alpha(k_{11} - k_{13}^2/k_{33})\right)\partial_x^2 u_1 - \frac{\lambda}{\lambda+2\mu}(\rho_e\omega^2\partial_x w_0 + \mu\partial_x^3 w_0)\right] = 0, \quad (4.7)$$

$$\mu\partial_x u_1 + (\rho_e + \alpha\rho_p)\omega^2 w_0 + \mu\partial_x^2 w_0 - \frac{h_e^2}{24(\lambda+2\mu)}\left[[\rho_e(2\lambda+3\mu) + 3\alpha\rho_p(\lambda+\mu)]\omega^2\partial_x u_1 + \mu(3\lambda+4\mu)\partial_x^3 u_1 + (\rho_e^2 + 3\alpha\rho_e\rho_p)\omega^4 w_0 - [\rho_e(\lambda-\mu) - 3\alpha\rho_p\mu]\omega^2\partial_x^2 w_0 - \lambda\mu\partial_x^4 w_0\right] = \frac{\alpha\rho_p\omega^2 e_{z3}}{2k_{33}}\Delta V. \quad (4.8)$$

The displacements in the piezoelectric and elastic interval are collected in vectors like

$$\mathbf{u}^{(1)} = \begin{pmatrix} w_0^{(1)} \\ u_1^{(1)} \end{pmatrix}, 0 \leqslant x \leqslant L_\mathrm{p}, \quad \mathbf{u}^{(2)} = \begin{pmatrix} w_0^{(2)} \\ u_1^{(2)} \end{pmatrix}, L_\mathrm{p} < x \leqslant L_\mathrm{e}.$$

To find the homogenous solution in the piezoelectric interval, $\mathbf{u}^{(1)} = \mathrm{e}^{\lambda x}\mathbf{a}$ is inserted into Eqs. (4.7) and (4.8) with no source term, which gives a homogenous system of two equations in the two unknowns a_1 and a_2, which are the components of $\mathbf{a}$. Putting the system determinant to zero gives an equation of the sixth degree in λ. For each solution λ_j, $j = 1, \ldots, 6$, the corresponding $(a_1)_j$ and $(a_2)_j$ can then be solved for. A particular solution is find by inserting a constant field $\mathbf{K}$ into Eqs. (4.7) and (4.8) and solving. The general solution for the mechanical field in the piezoelectric interval can then be written

$$\mathbf{u}^{(1)} = \sum_{j=1}^{6} A_j e^{\lambda_j x}\mathbf{a}_j + \mathbf{K}, \tag{4.9}$$

where A_j, $j = 1, \ldots, 6$, are constants to be determined.

For the elastic interval the assumption $\mathbf{u}^{(2)} = \mathrm{e}^{\mu x}\mathbf{b}$ is inserted into Eqs. (4.7) and (4.8) with $\alpha = 0$, which gives a homogenous system of equations. There will then be four solutions for μ and the general solution for the mechanical field in the elastic interval can be written

$$\mathbf{u}^{(2)} = \sum_{j=1}^{4} B_j e^{\mu_j x}\mathbf{b}_j, \tag{4.10}$$

where B_j, $j = 1, \ldots, 4$, are constants to be determined.

There are a total of 10 unknown constants and these are determined by the symmetry, interface and boundary conditions. The power series expansions (4.3) and (4.4) are inserted into these conditions and identification of equal powers of z gives an infinite number of equations. As the plate equations are given to quadratic order in h_e, only conditions that involve no other expansion functions than those up to quadratic order are kept. These are u_1, w_0 and w_2. Furthermore, as expansion functions up to quadratic order are used, only conditions up to quadratic order in z are kept. To eliminate w_2 the recursion relation (3.9) is used. The described method of selection results in 10 conditions which are given below.

The symmetry condition that $u^{(1)} = 0$ at $x = 0$ gives

$$u_1^{(1)} = 0, \quad x = 0, \tag{4.11}$$

while the symmetry condition that $\partial_x w^{(1)} = 0$ at $x = 0$ gives the following two equations

$$\partial_x w_0^{(1)} = 0, \quad x = 0, \tag{4.12}$$

$$(\lambda + \mu)\partial_x^2 u_1^{(1)} + \rho_\mathrm{e}\omega^2 \partial_x w_0^{(1)} + \mu\partial_x^3 w_0^{(1)} = 0, \quad x = 0. \tag{4.13}$$

Eqs. (4.11) and (4.12) together correspond to zero angle in the middle of the plate and zero shear force, while Eq. (4.13) has no obvious interpretation, but can be seen as representing zero shear stress at every point along the symmetry line.

The boundary conditions that $u^{(2)} = 0$ and $T_{xz}^{(2)} = 0$ at $x = L_\mathrm{e}$ give

$$u_1^{(2)} = 0, \quad x = L_\mathrm{e}, \tag{4.14}$$

$$u_1^{(2)} + \partial_x w_0^{(2)} = 0, \quad x = L_\mathrm{e}. \tag{4.15}$$

Eqs. (4.14) and (4.15) together correspond to zero angle in the middle of the plate and zero shear force.

The interface condition that $u^{(1)} = u^{(2)}$ at $x = L_\mathrm{p}$ gives

$$u_1^{(1)} = u_1^{(2)}, \quad x = L_\mathrm{p}, \tag{4.16}$$

while the interface condition that $w^{(1)} = w^{(2)}$ at $x = L_\mathrm{p}$ gives the following two equations:

$$w_0^{(1)} = w_0^{(2)}, \quad x = L_\mathrm{p}, \tag{4.17}$$

$$(\lambda + \mu)\partial_x u_1^{(1)} + \rho_\mathrm{e}\omega^2 w_0^{(1)} + \mu\partial_x^2 w_0^{(1)} = (\lambda + \mu)\partial_x u_1^{(2)} + \rho_\mathrm{e}\omega^2 w_0^{(2)} + \mu\partial_x^2 w_0^{(2)}, \quad x = L_\mathrm{p}. \tag{4.18}$$

The interface conditions that $T_{xx}^{(1)} = T_{xx}^{(2)}$ and $T_{xz}^{(1)} = T_{xz}^{(2)}$ at $x = L_\mathrm{p}$ give

$$\mu(3\lambda + 4\mu)\partial_x u_1^{(1)} - \rho_\mathrm{e}\omega^2\lambda w_0^{(1)} - \lambda\mu\partial_x^2 w_0^{(1)} = \mu(3\lambda + 4\mu)\partial_x u_1^{(2)} - \rho_\mathrm{e}\omega^2\lambda w_0^{(2)} - \lambda\mu\partial_x^2 w_0^{(2)}, \quad x = L_\mathrm{p}, \tag{4.19}$$

$$u_1^{(1)} + \partial_x w_0^{(1)} = u_1^{(2)} + \partial_x w_0^{(2)}, \quad x = L_\mathrm{p}. \tag{4.20}$$

Eq. (4.16) together with Eq. (4.20) represent continuity of angle in the middle of the plate and continuity of shear force. Eq. (4.17) corresponds to continuity of vertical displacement in the middle of the plate, while Eq. (4.18) can be seen as representing continuity of vertical displacement at every point along the interface. Eq. (4.19) represents continuity of bending moment.

Insertion of Eqs. (4.9) and (4.10) into Eqs. (4.11)–(4.20) gives a linear system of equations and the 10 unknown constants can then be solved for. The displacement fields are then given by Eqs. (4.9) and (4.10).

5. Exact solution

In this section the exact solution to the problem described in Section 2 is determined by use of the three equations of motion ((2.6)–(2.8)). All fields will be described in a coordinate system with the x axis along the interface between the two layers, according to Fig. 1.

Due to the boundary conditions at $x = \pm L_\mathrm{p}$ and $x = \pm L_\mathrm{e}$, Eqs. (2.19)–(2.23), and the fact that the solution must be symmetric in x, the fields in the piezoelectric and elastic layer are expanded in trigonometric Fourier series in the following way:

$$u^\mathrm{p}(x,z) = \sum_{m=1}^{\infty} u_m^\mathrm{p}(z)\sin(q_m^\mathrm{p}x), \tag{5.1}$$

$$w^\mathrm{p}(x,z) = \sum_{m=0}^{\infty} w_m^\mathrm{p}(z)\cos(q_m^\mathrm{p}x), \tag{5.2}$$

$$\Phi(x,z) = \sum_{m=0}^{\infty} \Phi_m(z)\cos(q_m^\mathrm{p}x), \tag{5.3}$$

$$u(x,z) = \sum_{m=1}^{\infty} u_m(z)\sin(q_m^\mathrm{e}x), \tag{5.4}$$

$$w(x,z) = \sum_{m=0}^{\infty} w_m(z)\cos(q_m^\mathrm{e}x), \tag{5.5}$$

where $q_m^\mathrm{p} = m\pi/L_\mathrm{p}$ and $q_m^\mathrm{e} = m\pi/L_\mathrm{e}$.

For the piezoelectric layer Eqs. (5.1)–(5.3) are inserted into the three equations of motion (2.6)–(2.8), which then are reduced to a set of ordinary differential equations in z for each m. For $m = 0$ the solution is

$$w_0^\mathrm{p}(z) = C_{01}\cos(k_0^\mathrm{p}z) + D_{01}\sin(k_0^\mathrm{p}z), \tag{5.6}$$

$$\Phi_0(z) = \frac{e_{z3}}{\epsilon_{zz}}[C_{01}\cos(k_0^\mathrm{p}z) + D_{01}\sin(k_0^\mathrm{p}z)] + C_{02} + D_{02}z, \tag{5.7}$$

where C_{01}, D_{01}, C_{02} and D_{02} are unknown constants and the stiffened wave number is $k_0^\mathrm{p} = \omega\sqrt{\rho_\mathrm{p}/\bar{k}_{33}}$ with $\bar{k}_{33} = k_{33} + e_{z3}^2/\epsilon_{zz}$. For $m = 1, 2, \ldots$, the horizontal displacement u_m also enters and the solution can be written

$$u_m^{\mathrm{p}}(z) = \sum_{n=1}^{3} \alpha_{mn}[C_{mn}\sinh(p_{mn}^{\mathrm{p}} z) + D_{mn}\cosh(p_{mn}^{\mathrm{p}} z)], \tag{5.8}$$

$$w_m^{\mathrm{p}}(z) = \sum_{n=1}^{3} \beta_{mn}[C_{mn}\cosh(p_{mn}^{\mathrm{p}} z) + D_{mn}\sinh(p_{mn}^{\mathrm{p}} z)], \tag{5.9}$$

$$\Phi_m(z) = \sum_{n=1}^{3} \gamma_{mn}[C_{mn}\cosh(p_{mn}^{\mathrm{p}} z) + D_{mn}\sinh(p_{mn}^{\mathrm{p}} z)], \tag{5.10}$$

where p_{mn}^{p}, α_{mn}, β_{mn} and γ_{mn} are determined from

$$[\rho_{\mathrm{p}}\omega^2 - k_{11}(q_m^{\mathrm{p}})^2 + k_{44}(p_m^{\mathrm{p}})^2]\alpha_m - (k_{13}+k_{44})q_m^{\mathrm{p}} p_m^{\mathrm{p}}\beta_m - (e_{x5}+e_{z1})q_m^{\mathrm{p}} p_m^{\mathrm{p}}\gamma_m = 0, \tag{5.11}$$

$$(k_{13}+k_{44})q_m^{\mathrm{p}} p_m^{\mathrm{p}}\alpha_m + [\rho_{\mathrm{p}}\omega^2 + k_{33}(p_m^{\mathrm{p}})^2 - k_{44}(q_m^{\mathrm{p}})^2]\beta_m + [e_{z3}(p_m^{\mathrm{p}})^2 - e_{x5}(q_m^{\mathrm{p}})^2]\gamma_m = 0, \tag{5.12}$$

$$(e_{x5}+e_{z1})q_m^{\mathrm{p}} p_m^{\mathrm{p}}\alpha_m + [e_{z3}(p_m^{\mathrm{p}})^2 - e_{x5}(q_m^{\mathrm{p}})^2]\beta_m + [\epsilon_{xx}(q_m^{\mathrm{p}})^2 - \epsilon_{zz}(p_m^{\mathrm{p}})^2]\gamma_m = 0. \tag{5.13}$$

For this homogenous system to have a solution, the determinant must equal zero, which yields a third order equation in $(p_m^{\mathrm{p}})^2$. Only keeping solutions with $Re(p_m^{\mathrm{p}}) \geqslant 0$ gives three $p_m^{\mathrm{p}} = p_{mn}^{\mathrm{p}}$, $n = 1,2,3$, and the corresponding α_{mn}, β_{mn} and γ_{mn} can then be solved for, using some convenient normalization.

For the elastic layer Eqs. (5.4) and (5.5) are inserted into Eqs. (2.6) and (2.7) with all piezoelectric coupling constants put to zero and specialization to isotropic elastic material. A set of ordinary differential equations in z for each m is obtained and for $m = 0$ the solution is

$$w_0(z) = E_{01}\cos(k_0^{\mathrm{e}} z) + F_{01}\sin(k_0^{\mathrm{e}} z), \tag{5.14}$$

where E_{01} and F_{01} are unknown constants and the wave number is $k_0^{\mathrm{e}} = \omega\sqrt{\rho_{\mathrm{e}}/(\lambda+2\mu)}$. For $m = 1,2,\ldots$, the solution can be written

$$u_m(z) = \sum_{n=1}^{2} a_{mn}[E_{mn}\sinh(p_{mn}^{\mathrm{e}} z) + F_{mn}\cosh(p_{mn}^{\mathrm{e}} z)], \tag{5.15}$$

$$w_m(z) = \sum_{n=1}^{2} b_{mn}[E_{mn}\cosh(p_{mn}^{\mathrm{e}} z) + F_{mn}\sinh(p_{mn}^{\mathrm{e}} z)], \tag{5.16}$$

where $p_{m1}^{\mathrm{e}} = \sqrt{(q_m^{\mathrm{e}})^2 - \rho_{\mathrm{e}}\omega^2/\mu}$, $p_{m2}^{\mathrm{e}} = \sqrt{(q_m^{\mathrm{e}})^2 - \rho_{\mathrm{e}}\omega^2/(\lambda+2\mu)}$, $a_{m1}/b_{m1} = -p_{m1}^{\mathrm{e}}/q_m^{\mathrm{e}}$ and $a_{m2}/b_{m2} = -q_m^{\mathrm{e}}/p_{m2}^{\mathrm{e}}$.

The unknown constants C_{mn}, D_{mn}, E_{mn} and F_{mn} are determined below by the boundary and interface conditions (2.9)–(2.18). To get a finite number of unknowns the Fourier series have to be truncated at some level. In the piezoelectric layer terms up to $m = M_{\mathrm{p}}$ are kept and in the elastic layer terms up to $m = M_{\mathrm{e}}$ are kept, where M_{p} and M_{e} are finite integers, chosen in some appropriate manner. The more terms that are taken into account, the better results are expected.

The two boundary conditions (2.9) and (2.10) of vanishing stresses at the bottom of the elastic layer give

$$\sum_{n=1}^{2} \zeta_{mn}[E_{mn}\cosh(p_{mn}^{\mathrm{e}} h_{\mathrm{e}}) - F_{mn}\sinh(p_{mn}^{\mathrm{e}} h_{\mathrm{e}})] = 0, \tag{5.17}$$

$$E_{01}\sin(k_0^{\mathrm{e}} h_{\mathrm{e}}) + F_{01}\cos(k_0^{\mathrm{e}} h_{\mathrm{e}}) = 0, \tag{5.18}$$

$$\sum_{n=1}^{2} \varepsilon_{mn}[E_{mn}\sinh(p_{mn}^{\mathrm{e}} h_{\mathrm{e}}) - F_{mn}\cosh(p_{mn}^{\mathrm{e}} h_{\mathrm{e}})] = 0, \tag{5.19}$$

where $m = 1,2,\ldots,M_{\mathrm{e}}$ and

$$\zeta_{mn} = \mu(a_{mn}p_{mn}^{\mathrm{e}} - b_{mn}q_m^{\mathrm{e}}),$$
$$\varepsilon_{mn} = \lambda a_{mn}q_m^{\mathrm{e}} + (\lambda+2\mu)b_{mn}p_{mn}^{\mathrm{e}}.$$

The two boundary conditions (2.11) and (2.12) of vanishing stresses at the top of the piezoelectric layer give

$$\sum_{n=1}^{3} \eta_{mn}[C_{mn}\cosh(p_{mn}^{\mathrm{p}} h_{\mathrm{p}}) + D_{mn}\sinh(p_{mn}^{\mathrm{p}} h_{\mathrm{p}})] = 0, \tag{5.20}$$

$$\bar{k}_{33}k_0^{\mathrm{p}}[-C_{01}\sin(k_0^{\mathrm{p}} h_{\mathrm{p}}) + D_{01}\cos(k_0^{\mathrm{p}} h_{\mathrm{p}})] + e_{z3}D_{02} = 0, \tag{5.21}$$

$$\sum_{n=1}^{3} \xi_{mn}[C_{mn}\sinh(p_{mn}^{\mathrm{p}} h_{\mathrm{p}}) + D_{mn}\cosh(p_{mn}^{\mathrm{p}} h_{\mathrm{p}})] = 0, \tag{5.22}$$

where $m = 1,2,\ldots,M_{\mathrm{p}}$, and

$$\eta_{mn} = k_{55}\alpha_{mn}p_{mn}^{\mathrm{p}} - k_{55}\beta_{mn}q_m^{\mathrm{p}} - e_{x5}\gamma_{mn}q_m^{\mathrm{p}},$$
$$\xi_{mn} = k_{13}\alpha_{mn}q_m^{\mathrm{p}} + k_{33}\beta_{mn}p_{mn}^{\mathrm{p}} + e_{z3}\gamma_{mn}p_{mn}^{\mathrm{p}}.$$

Note that the boundary conditions on the shear stresses, T_{xz} and T_{xz}^{p}, are trivially satisfied for $m = 0$.

The electric boundary condition (2.13) at the top of the piezoelectric layer gives

$$\frac{e_{z3}}{\epsilon_{zz}}[C_{01}\cos(k_0^{\mathrm{p}} h_{\mathrm{p}}) + D_{01}\sin(k_0^{\mathrm{p}} h_{\mathrm{p}})] + C_{02} + D_{02}h_{\mathrm{p}} = V_1, \tag{5.23}$$

$$\sum_{n=1}^{3} \gamma_{mn}[C_{mn}\cosh(p_{mn}^{\mathrm{p}} h_{\mathrm{p}}) + D_{mn}\sinh(p_{mn}^{\mathrm{p}} h_{\mathrm{p}})] = 0, \tag{5.24}$$

where $m = 1,2,\ldots,M_{\mathrm{p}}$.

The electric boundary condition (2.18) at the bottom of the piezoelectric layer gives

$$\frac{e_{z3}}{\epsilon_{zz}}C_{01} + C_{02} = V_0, \tag{5.25}$$

$$\sum_{n=1}^{3} \gamma_{mn}C_{mn} = 0, \tag{5.26}$$

where $m = 1,2,\ldots,M_{\mathrm{p}}$.

The interface conditions (2.14) and (2.15) of continuity of stress give, after truncation

$$\sum_{m=1}^{M_{\mathrm{e}}}\sum_{n=1}^{2} \zeta_{mn}E_{mn}\sin(q_m^{\mathrm{e}} x) = \begin{cases} \sum_{m=1}^{M_{\mathrm{p}}}\sum_{n=1}^{3} \eta_{mn}C_{mn}\sin(q_m^{\mathrm{p}} x), & |x| \leqslant L_{\mathrm{p}} \\ 0, & |x| > L_{\mathrm{p}} \end{cases}, \tag{5.27}$$

$$\sum_{m=0}^{M_{\mathrm{e}}}\sum_{n=1}^{2} \varepsilon_{mn}F_{mn}\cos(q_m^{\mathrm{e}} x) = \begin{cases} \sum_{m=0}^{M_{\mathrm{p}}}\sum_{n=1}^{3} \xi_{mn}D_{mn}\cos(q_m^{\mathrm{p}} x), & |x| \leqslant L_{\mathrm{p}} \\ 0, & |x| > L_{\mathrm{p}} \end{cases}, \tag{5.28}$$

where $m = 0$ is incorporated by defining

$$\varepsilon_{01} = (\lambda+2\mu)k_0^{\mathrm{e}}, \quad \varepsilon_{02} = 0,$$
$$\xi_{01} = \bar{k}_{33}k_0^{\mathrm{p}}, \quad \xi_{02} = e_{z3}, \quad \xi_{03} = 0.$$

Eqs. (5.27) and (5.28) are multiplied by the eigenfunctions $\sin(q_k^{\mathrm{e}} x)$ and $\cos(q_k^{\mathrm{e}} x)$, respectively, and are then integrated along the interval $-L_{\mathrm{e}} \leqslant x \leqslant L_{\mathrm{e}}$. Using the orthogonality property of the eigenfunctions and switching indices then give

$$\sum_{n=1}^{2} \zeta_{mn}E_{mn} = \frac{1}{L_{\mathrm{e}}}\sum_{k=1}^{M_{\mathrm{p}}}\sum_{n=1}^{3} \eta_{kn}C_{kn}\int_{-L_{\mathrm{p}}}^{L_{\mathrm{p}}} \sin(q_k^{\mathrm{p}} x)\sin(q_m^{\mathrm{e}} x)\mathrm{d}x, \tag{5.29}$$

$$(\lambda+2\mu)k_0^{\mathrm{e}}F_{01} = \frac{L_{\mathrm{p}}}{L_{\mathrm{e}}}(\bar{k}_{33}k_0^{\mathrm{p}}D_{01} + e_{z3}D_{02}), \tag{5.30}$$

$$\sum_{n=1}^{2} \varepsilon_{mn}F_{mn} = \frac{1}{L_{\mathrm{e}}}\sum_{k=0}^{M_{\mathrm{p}}}\sum_{n=1}^{3} \xi_{kn}D_{kn}\int_{-L_{\mathrm{p}}}^{L_{\mathrm{p}}} \cos(q_k^{\mathrm{p}} x)\cos(q_m^{\mathrm{e}} x)\mathrm{d}x, \tag{5.31}$$

where $m = 1,2,\ldots,M_{\mathrm{e}}$.

The interface conditions (2.16) and (2.17) of continuity of displacement give, after truncation

$$\sum_{m=1}^{M_e}\sum_{n=1}^{2} a_{mn}F_{mn}\sin(q_m^e x) = \sum_{m=1}^{M_p}\sum_{n=1}^{3} \alpha_{mn}D_{mn}\sin(q_m^p x), \quad |x| \leqslant L_p, \tag{5.32}$$

$$\sum_{m=0}^{M_e}\sum_{n=1}^{2} b_{mn}E_{mn}\cos(q_m^e x) = \sum_{m=0}^{M_p}\sum_{n=1}^{3} \beta_{mn}C_{mn}\cos(q_m^p x), \quad |x| \leqslant L_p, \tag{5.33}$$

where $m = 0$ is incorporated by defining

$$b_{01} = 1, \quad b_{02} = 0,$$
$$\beta_{01} = 1, \quad \beta_{02} = 0, \quad \beta_{03} = 0.$$

Multiplication by the eigenfunctions $\sin(q_k^p x)$ and $\cos(q_k^p x)$, respectively, and integration along the interval $-L_p \leqslant x \leqslant L_p$ give, after the use of orthogonality and an index switch

$$\sum_{n=1}^{3} \alpha_{mn}D_{mn} = \frac{1}{L_p}\sum_{k=1}^{M_e}\sum_{n=1}^{2} a_{kn}F_{kn}\int_{-L_p}^{L_p} \sin(q_k^e x)\sin(q_m^p x)\mathrm{d}x, \tag{5.34}$$

$$C_{01} = E_{01} + \frac{1}{2L_p}\sum_{k=1}^{M_e}\sum_{n=1}^{2} b_{kn}E_{kn}\int_{-L_p}^{L_p} \cos(q_k^e x)\mathrm{d}x, \tag{5.35}$$

$$\sum_{n=1}^{3} \beta_{mn}C_{mn} = \frac{1}{L_p}\sum_{k=1}^{M_e}\sum_{n=1}^{2} b_{kn}E_{kn}\int_{-L_p}^{L_p} \cos(q_k^e x)\cos(q_m^p x)\mathrm{d}x, \tag{5.36}$$

where $m = 1, 2, \ldots, M_p$.

Eqs. (5.17)–(5.26), (5.29)–(5.31) and (5.34)–(5.36) form a system of $(6 + 6M_p + 4M_e)$ linear equations with just as many unknowns. These are C_{01}, C_{02}, D_{01}, D_{02}, C_{mn}, D_{mn}, where $m = 1, 2, \ldots, M_p$, $n = 1, 2, 3$, belonging to the piezoelectric layer and E_{01}, F_{01}, E_{mn}, F_{mn}, where $m = 1, 2, \ldots, M_e$, $n = 1, 2$, belonging to the elastic layer. This system is straightforward to solve, whereafter the displacement field in the elastic layer is obtained from Eqs. (5.4) and (5.5) with truncations.

6. Numerical results

In this section numerical results for the problem described in Section 2 are given. Comparisons are made between the solution with plate equations described in Section 3, the solution with equivalent boundary conditions described in Section 4 and the exact solution described in Section 5. The main goals are to investigate the accuracy of the plate equations and to compare the two approximate theories. Only the vertical displacement w in the middle of the elastic layer ($z = 0$) is investigated. The reason why the horizontal displacement u is left out is that the exact solution of this displacement component converges extremely slowly due to a singularity at $x = L_p$, $z = 0$, see Fig. 1. It has been investigated how well the exact solution fulfils the boundary and interface conditions at the top and the bottom of each layer, Eqs. (2.10)–(2.18), and it can be certified that they are all fulfilled very well for a sufficient number of terms in the Fourier series, with the only exception of continuity of horizontal displacement between the two layers at the positions $x = \pm L_p$, $z = 0$. There the horizontal displacement in the piezoelectric layer is forced to make a very steep dip to zero due to boundary condition (2.22), but the horizontal displacement in the elastic layer is not close to zero at this point. It has also been observed that the shear stresses T_{xz} and T_{xz}^p in the elastic and piezoelectric layer, respectively, become very big as x approach $\pm L_p$ for $z = 0$. It should be mentioned that the horizontal displacement u is much smaller than the vertical displacement w, so the absolute error in u is not very much larger than the absolute error in w, even if the relative error in u is much larger than the relative error in w. Another thing worth to mention is that there is also convergence problems for very low frequencies. A possible reason to this is that $\Omega = 0$ is actually an eigenfrequency, as there is a rigid body translation mode in the vertical direction. To obtain sufficient convergence in the exact solution of w, the number of terms to use in the Fourier series expansions of the displacements in the elastic layer is chosen to $M_e = 100$. Then the number of terms to use in the Fourier series expansions of the fields in the piezoelectric layer is chosen so that the fraction between the number of terms in the elastic and piezoelectric layer roughly equals the length fraction between the layers, i.e. $M_p/M_e \approx L_p/L_e$, as a longer layer holds more oscillations than a shorter layer.

The piezoelectric layer is PZT-2 (Lead Zirconate Titanate), which is of symmetry class *6mm*, with material constants, see Auld (1990) $\rho_p = 7600\ \mathrm{kg/m^3}$, $k_{11} = 135$ GPa, $k_{13} = 68.1$ GPa, $k_{33} = 113$ GPa, $k_{44} = 22.2$ GPa, $e_{x5} = 9.8\ \mathrm{C/m^2}$, $e_{z1} = -1.9\ \mathrm{C/m^2}$, $e_{z3} = 9.0\ \mathrm{C/m^2}$, $\epsilon_{xx} = 504\epsilon_0$, and $\epsilon_{zz} = 260\epsilon_0$. Here $\epsilon_0 = 8.854 \cdot 10^{-12}$ C/Vm is the dielectric permittivity of free space. The elastic layer is isotropic steel with density $\rho_e = 7870\ \mathrm{kg/m^3}$, Young's modulus $E = 210$ GPa and Poisson's ratio $\nu = 0.3$. The vertical displacement in the elastic layer is measured with the dimensionless variable $W = we_{z3}/(\epsilon_{zz}\Delta V)$. Also a dimensionless frequency $\Omega = \omega h\sqrt{\rho_e/(\lambda + 2\mu)}$ is introduced, where $h = h_e + h_p$ is the total thickness of the plate. There are a couple of geometric parameters that are varied in the numerical investigations: the thickness ratio between the layers, $\alpha = h_p/h_e$, the ratio between the total plate thickness and the length of the elastic layer, $\beta = h/(2L_e)$, and the length ratio between the layers, $\gamma = L_p/L_e$.

In the following, numerical investigations of the vertical displacement W in the middle of the elastic layer ($z = 0$) is compared between solutions with plate equations (given by full-drawn lines in the figures), equivalent boundary conditions (given by dashed lines) and exact theory (given by dotted lines). Some of the figures show the vertical displacement in the middle of the elastic layer ($z = 0$) at $x = 0$ as a function of frequency, Ω, and other figures show the vertical displacement in the middle of the elastic layer as a function of x/L_e for a certain frequency.

Fig. 3 shows the vertical displacement in the middle of the elastic layer ($z = 0$) at $x = 0$ as a function of frequency. The piezoelectric layer thickness is one fourth of the total plate thickness ($\alpha = 1/3$), the total plate thickness is one tenth of the length of the elastic layer ($\beta = 1/10$) and the piezoelectric layer is half as long as the elastic layer ($\gamma = 1/2$). As can be seen from the figure the displacement at some frequencies goes to infinity, which means that there is an eigenfrequency. The figure shows that the two approximate theories yield accurate results at low frequencies and the first three eigenfrequencies are quite well predicted by both of them. Near the second eigenfrequency the displacements predicted by the approximate theories diverge from the exact solution, but for higher frequencies they get closer again. In general the magnitude of the approximate solutions is not accurate close to an eigenfrequency. The first eigenfrequency belongs to an approximately antisymmetric mode and is close to the first eigenfrequency of a Kirchhoff plate with the same dimensions as the elastic layer; $\Omega_1 \approx 0.077$. The second eigenfrequency is also an approximately antisymmetric one and the corresponding Kirchhoff frequency is $\Omega_2 \approx 0.31$. The third eigenfrequency is not well predicted by Kirchhoff theory, but it is still an almost antisymmetric eigenfrequency as the equivalent boundary condition solution, only regarding antisymmetric motion, goes to infinity at this frequency. For frequencies above $\Omega = 0.6$ the results are no longer accurate. As the results are rather good for frequencies around $\Omega = 0.45$, Fig. 4 shows the vertical displacement W in the middle of the elastic layer as a function of x/L_e for the same case as in Fig. 3 and that specific frequency. As can be seen the curves coincide rather well, but it should be noticed that in this kind of plots it is very much depending on frequency how well the curves agree.

Fig. 5 shows the same situation as Fig. 3 but for a thinner plate with a total thickness that is 1/40 of the length of the elastic layer

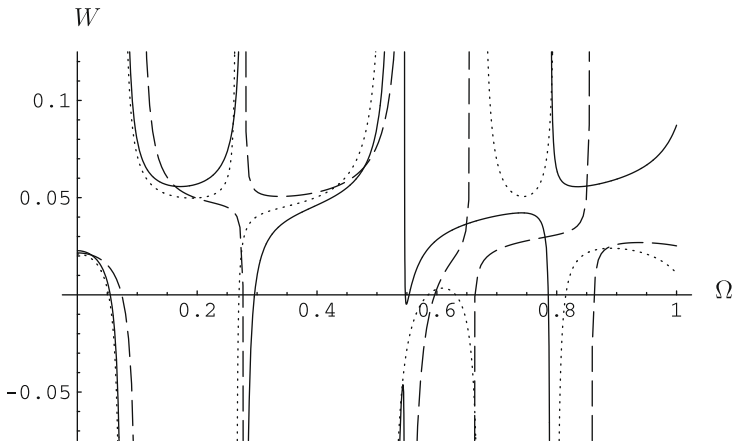

Fig. 3. The vertical displacement in the middle of the elastic layer at $x = 0$, comparing plate equation (full-drawn), equivalent boundary condition (dotted) and exact (dashed) solutions for $\alpha = 1/3$, $\beta = 1/10$, $\gamma = 1/2$.

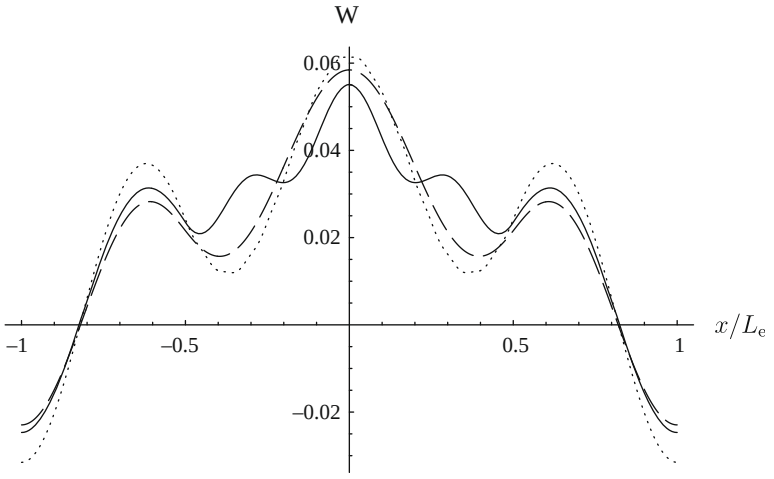

Fig. 4. The vertical displacement in the middle of the elastic layer, comparing plate equation (full-drawn), equivalent boundary condition (dotted) and exact (dashed) solutions for $\Omega = 0.45$, $\alpha = 1/3$, $\beta = 1/10$, $\gamma = 1/2$.

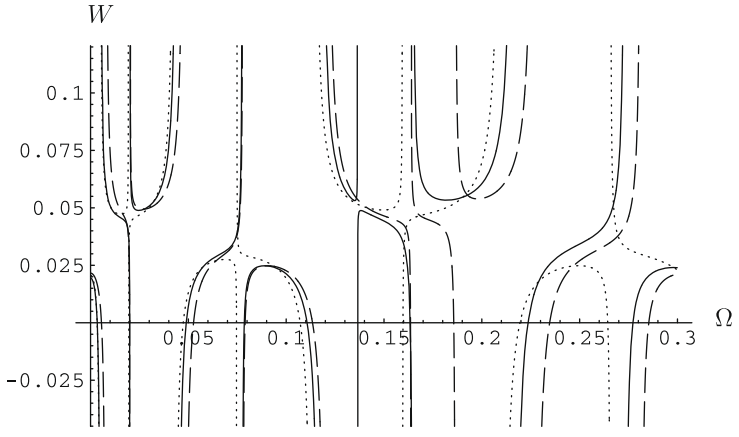

Fig. 5. The vertical displacement in the middle of the elastic layer at $x = 0$, comparing plate equation (full-drawn), equivalent boundary condition (dotted) and exact (dashed) solutions for $\alpha = 1/3$, $\beta = 1/40$, $\gamma = 1/2$.

($\beta = 1/40$). As a thinner plate has more eigenfrequencies below a given frequency than a thicker plate, this figure is plotted for a shorter frequency interval. For frequencies below $\Omega = 0.17$ the results are very good, but the approximate curves are quite accurate over the whole frequency interval. The first five eigenfrequencies are well predicted by both approximate theories, which is more than in the previous case with a thicker plate. Fig. 6 shows the vertical displacement as a function of x/L_e for this case and the fre-

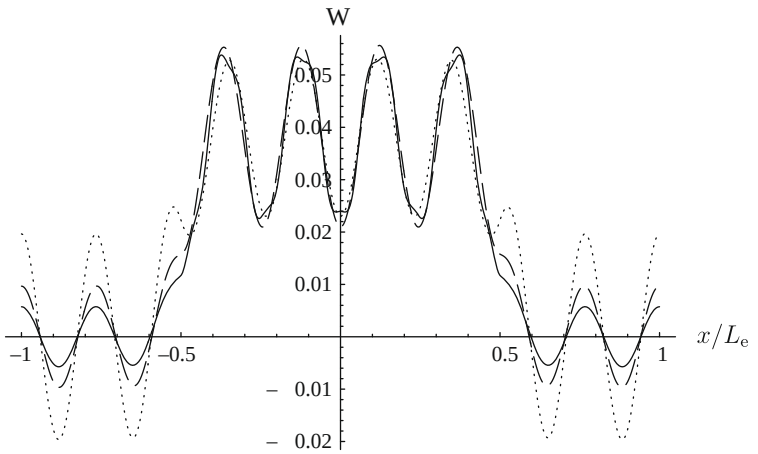

Fig. 6. The vertical displacement in the middle of the elastic layer, comparing plate equation (full-drawn), equivalent boundary condition (dotted) and exact (dashed) solutions for $\Omega = 0.3$, $\alpha = 1/3$, $\beta = 1/40$, $\gamma = 1/2$.

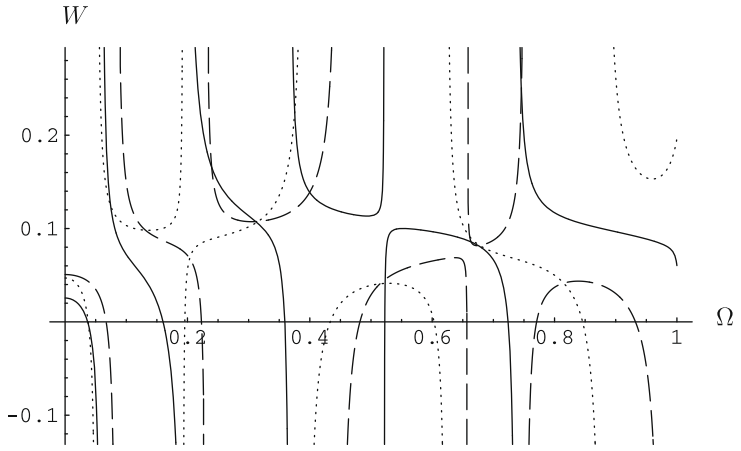

Fig. 7. The vertical displacement in the middle of the elastic layer at $x = 0$, comparing plate equation (full-drawn), equivalent boundary condition (dotted) and exact (dashed) solutions for $\alpha = 1$, $\beta = 1/10$, $\gamma = 1/2$.

quency $\Omega = 0.3$, which is a frequency where the three curves in Fig. 5 almost coincide. The agreement is good, especially for the plate equation solution.

Fig. 7 is similar to Fig. 3 but here both layers are of equal thickness ($\alpha = 1$). Both approximate theories yield curves that are less accurate than the curves in Fig. 3, where the piezoelectric layer is thinner. The plate equation solution yields bad results even for very low frequencies, while the equivalent boundary condition solution seems more accurate for low frequencies. For slightly higher frequencies though the equivalent boundary condition solution is even less accurate than the plate equation solution, so none of these theories is really applicable to this case. Both approximate theories predict the first two eigenfrequencies fairly well. For frequencies above $\Omega = 0.6$ none of the approximate theories are accurate at all. Fig. 8 shows the vertical displacement as a function of x/L_e for the same case as in Fig. 7 for the frequency $\Omega = 0.3$. The accuracy is good for the equivalent boundary condition solution, but the plate equation solution is less accurate. However, the results would not be that good for another choice of frequency.

Fig. 9 shows the same situation as Fig. 7 but for a thin plate, i.e. $\alpha = 1$, $\beta = 1/40$, $\gamma = 1/2$. Also here a shorter frequency interval is used. The results are better than for a thicker plate in the sense that more eigenfrequencies are quite well predicted. However, the results are less accurate than in Fig. 5 where the piezoelectric layer is thinner. The plate equation solution seems a bit better than the equivalent boundary condition solution, but none of the approximate theories seem really applicable to this case. Fig. 10 shows the vertical displacement as a function of x/L_e for this case and the frequency $\Omega = 0.3$. The approximate curves match the exact curve fairly well.

Fig. 11 is similar to Fig. 3, but shows results for a shorter piezoelectric layer ($\gamma = 1/5$). The equivalent boundary condition solution is better than the plate equation solution, but both theories yield very accurate results for frequencies below $\Omega = 0.3$. For frequencies above $\Omega = 0.6$ the results are not accurate at all. The first three eigenfrequencies are well predicted by both approximate theories. Observe that the accuracy of both approximate theories is better here than in Fig. 3, where the piezoelectric layer is longer. This shows that better results are obtained from the approximate theories when the piezoelectric layer is smaller. However, if the piezoelectric layer is very short, with unchanged value of β, the results will be less accurate again, as the piezoelectric layer will then not be thin in comparison to its length. Fig. 12 shows the vertical displacement as a function of x/L_e for the same case as in Fig. 11 for the frequency $\Omega = 0.2$. The agreement with the exact curve is good for both approximate curves.

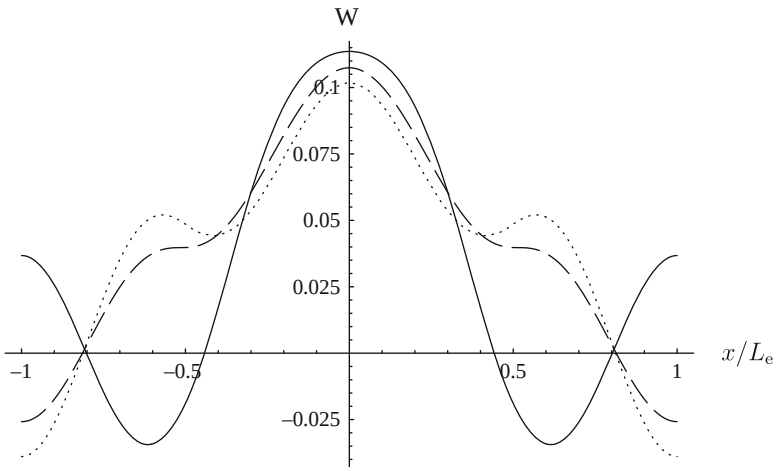

Fig. 8. The vertical displacement in the middle of the elastic layer, comparing plate equation (full-drawn), equivalent boundary condition (dotted) and exact (dashed) solutions for $\Omega = 0.3$, $\alpha = 1$, $\beta = 1/10$, $\gamma = 1/2$.

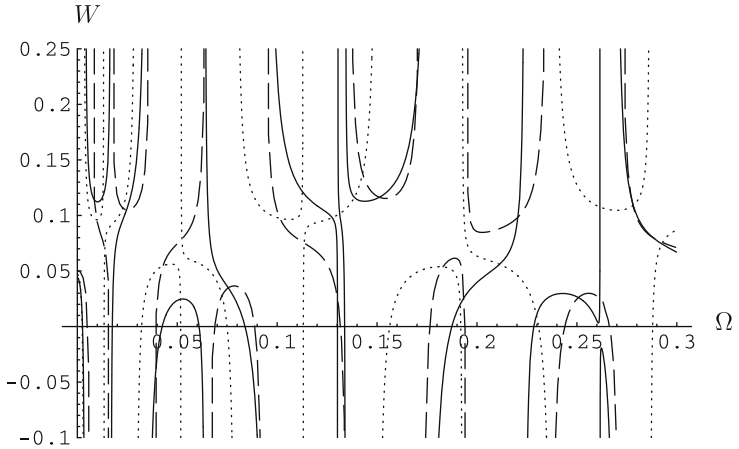

Fig. 9. The vertical displacement in the middle of the elastic layer at $x = 0$, comparing plate equation (full-drawn), equivalent boundary condition (dotted) and exact (dashed) solutions for $\alpha = 1$, $\beta = 1/40$, $\gamma = 1/2$.

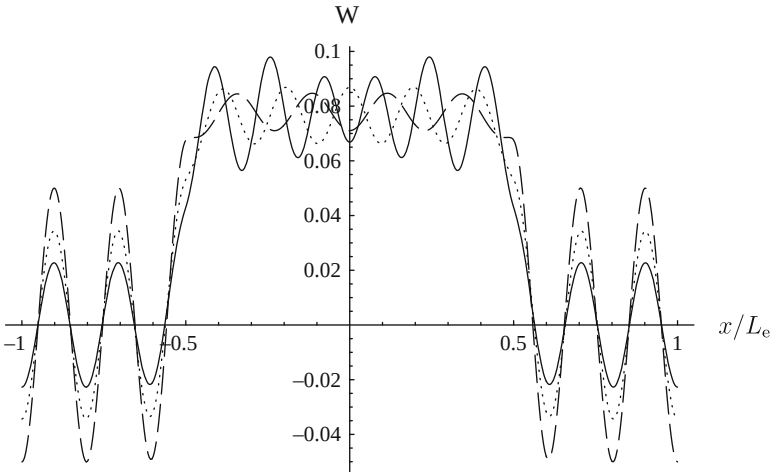

Fig. 10. The vertical displacement in the middle of the elastic layer, comparing plate equation (full-drawn), equivalent boundary condition (dotted) and exact (dashed) solutions for $\Omega = 0.3$, $\alpha = 1$, $\beta = 1/40$, $\gamma = 1/2$.

Fig. 13 also shows results for a short piezoelectric layer ($\gamma = 1/5$) but for a thin plate ($\beta = 1/40$). Both approximate theories agree very well with the exact solution and the results are better than in Fig. 5 where the piezoelectric layer is longer and Fig. 11 where the total plate is thicker. In this case the approximate solutions are accurate over the whole frequency interval

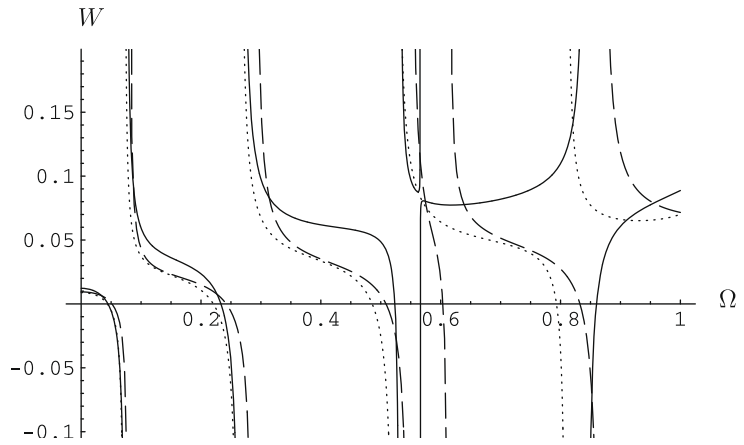

Fig. 11. The vertical displacement in the middle of the elastic layer at $x = 0$, comparing plate equation (full-drawn), equivalent boundary condition (dotted) and exact (dashed) solutions for $\alpha = 1/3$, $\beta = 1/10$, $\gamma = 1/5$.

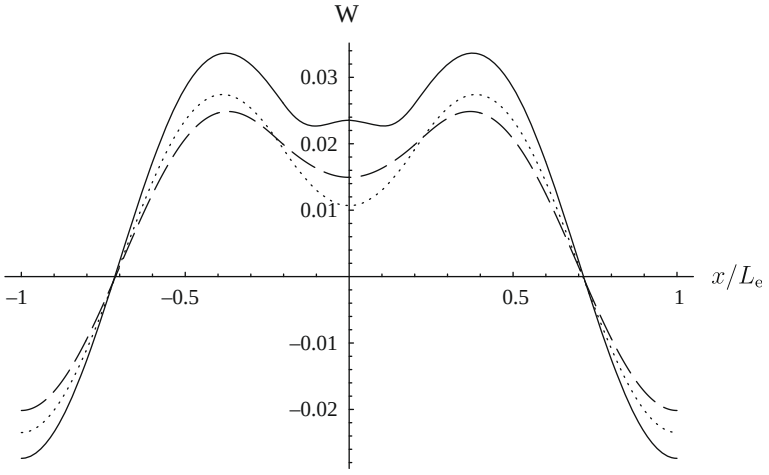

Fig. 12. The vertical displacement in the middle of the elastic layer, comparing plate equation (full-drawn), equivalent boundary condition (dotted) and exact (dashed) solutions for $\Omega = 0.2$, $\alpha = 1/3$, $\beta = 1/10$, $\gamma = 1/5$.

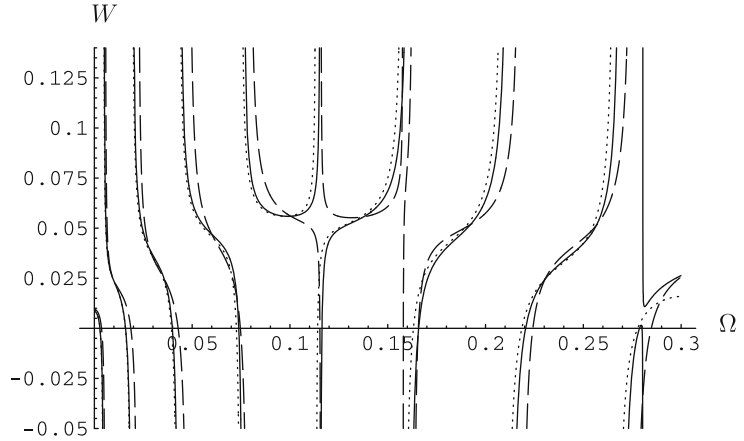

Fig. 13. The vertical displacement in the middle of the elastic layer at $x = 0$, comparing plate equation (full-drawn), equivalent boundary condition (dotted) and exact (dashed) solutions for $\alpha = 1/3$, $\beta = 1/40$, $\gamma = 1/5$.

and the first six eigenfrequencies are very well predicted by both of them. Fig. 14 shows the vertical displacement as a function of x/L_e for this case and the frequency $\Omega = 0.25$. The three curves agree very well.

It is hard to say something general about the differences in accuracy between the two approximate theories. In some cases the plate equation solution seems better than the equivalent boundary condition solution, but in other cases the relation is

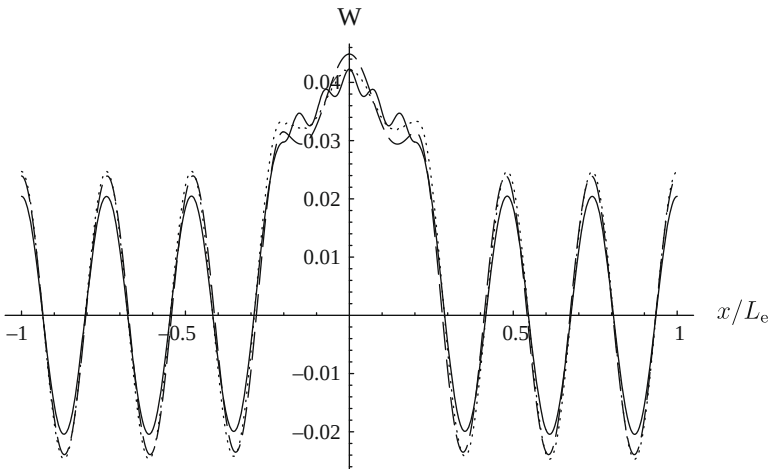

Fig. 14. The vertical displacement in the middle of the elastic layer, comparing plate equation (full-drawn), equivalent boundary condition (dotted) and exact (dashed) solutions for $\Omega = 0.25$, $\alpha = 1/3$, $\beta = 1/40$, $\gamma = 1/5$.

the opposite. The conclusion is that the two theories seem to be equally good. Another conclusion from the numerical investigations is that the approximate theories are not applicable for cases where the piezoelectric layer is of the same thickness as the elastic layer. It has to be thinner and accurate results seem to be obtained if the piezoelectric layer thickness is one fourth of the total plate thickness ($\alpha = 1/3$).

7. Concluding remarks

Plate equations for an elastic layer with a piezoelectric layer on top of it have previously been derived by the use of power series expansions in the thickness coordinate. Here it is shown how these plate equations can be used to solve a vibration problem with finite layers. The boundary conditions to combine with the plate equations are derived by inserting the power series expansions of the displacements into the physical boundary conditions at the sides of the elastic layer and identifying equal powers of the thickness coordinate.

Numerical comparisons of the vertical displacement in the middle of the elastic layer are made with two other theories; another approximate theory based on the same type of power series expansions where the piezoelectric layer is modeled as equivalent boundary conditions and exact theory. The two approximate theories are shown to be equally good and they both yield accurate results for thin plates and low frequencies if the piezoelectric layer thickness is not more than one fourth of the total plate thickness. In general better results are obtained when the piezoelectric layer is smaller if it is still thin in comparison to its length.

A possible application of the evaluated plate equations is as a starting point for the development of plate elements with piezoelectric layers, to be used in finite element codes. The equivalent boundary conditions provide another way to include piezoelectric layers into finite element computations. An advantage with the equivalent boundary conditions is that they are possible to apply to an elastic body in an already existing finite element program. Both approaches have the advantage of avoiding the modelling of a piezoelectric layer with many or very elongated elements, where the former may lead to numerical problems.

Acknowledgement

The present work is sponsored by the Swedish Research Council and this is gratefully acknowledged.

References

Auld, B., 1990. Acoustic Fields and Waves in Solids. Krieger, Malabar, FL.
Bisegna, P., Caruso, G., 2001. Evaluation of higher-order theories of piezoelectric plates in bending and in stretching. Int. J. Solids Struct. 38, 8805–8830.
Boström, A., Johansson, G., Olsson, P., 2001. On the rational derivation of a hierarchy of dynamic equations for a homogeneous, isotropic, elastic plate. Int. J. Solids Struct. 38, 2487–2501.
Boström, A., Zhang, B., 2005. In-plane P-SV waves from a piezoelectric strip actuator: exact versus effective boundary condition solutions. IEEE Trans. Ultrason. Ferroelectr. Freq. Control 52, 1594–1600.
Fernandes, A., Pouget, J., 2002. An accurate modelling of piezoelectric multi-layer plates. Eur. J. Mech. A – Solids 21, 629–651.
Fernandes, A., Pouget, J., 2006. Structural response of composite plates equipped with piezoelectric actuators. Comput. Struct. 84, 1459–1470.
Gopinathan, S., Varadan, V., Varadan, V., 2000. A review and critique of theories for piezoelectric laminates. Smart Mater. Struct. 9, 24–48.
Johansson, G., Niklasson, A., 2003. Approximate dynamic boundary conditions for a thin piezoelectric layer. Int. J. Solids Struct. 40, 3477–3492.
Kapuria, S., 2004. A coupled zig-zag third-order theory for piezoelectric hybrid cross-ply plates. J. Appl. Mech. Trans. ASME 71, 604–614.
Kapuria, S., Achary, G., 2005. A coupled zigzag theory for the dynamics of piezoelectric hybrid cross-ply plates. Arch. Appl. Mech. 75, 42–57.
Kochetkov, I., Rogacheva, N., 2005. Contact interaction of a piezoelectric actuator and elastic half-space. J. Appl. Math. Mech. 69, 792–804.
Kögl, M., Bucalem, M., 2005. A family of piezoelectric MITC plate elements. Comput. Struct. 83, 1277–1297.
Lim, C., Cheng, Z., Reddy, J., 2006. Natural frequencies of laminated piezoelectric plates with internal electrodes. Z. Angew. Math. Mech. 86, 410–420.
Lim, C., Lau, C., 2005. A new two-dimensional model for electro-mechanical response of thick laminated piezoelectric actuator. Int. J. Solids Struct. 42, 5589–5611.
Mauritsson, K., Boström, A., Folkow, P., 2008. Modelling of thin piezoelectric layers on plates. Wave Motion 45, 616–628.
Mindlin, R., 1951. Influence of rotatory inertia and shear on flexural motions of isotropic, elastic plates. J. Appl. Mech. 18, 31–38.
Raghavan, A., Cesnik, C., 2005. Finite-dimensional piezoelectric transducer modeling for guided wave based structural health monitoring. Smart Mater. Struct. 14, 1448–1461.
Robbins, D., Chopra, I., 2006. The effect of laminate kinematic assumptions on the global response of actuated plates. J. Int. Mater. Syst. Struct. 17, 273–299.
Tiersten, H., 1969. Linear Piezoelectric Plate Vibrations. Plenum, New York.
Vasques, C., Rodrigues, J., 2005. Coupled three-layered analysis of smart piezoelectric beams with different electric boundary conditions. Int. J. Numer. Meth. Engng. 62, 1488–1518.
Wang, J., Yang, J., 2000. Higher-order theories of piezoelectric plates and applications. Appl. Mech. Rev. 53, 87–99.
Wu, C., Lo, J., 2006. An asymptotic theory for dynamic response of laminated piezoelectric shells. Acta Mech. 183, 177–208.